



LUND UNIVERSITY

A Mode-III Crack Subjected to High-Strain Rates

Ståhle, P.

Published in:
Journal of the Mechanics and Physics of Solids

DOI:
[10.1016/0022-5096\(92\)80008-E](https://doi.org/10.1016/0022-5096(92)80008-E)

1992

Document Version:
Peer reviewed version (aka post-print)

[Link to publication](#)

Citation for published version (APA):
Ståhle, P. (1992). A Mode-III Crack Subjected to High-Strain Rates. *Journal of the Mechanics and Physics of Solids*, 40(3), 663-681. [https://doi.org/10.1016/0022-5096\(92\)80008-E](https://doi.org/10.1016/0022-5096(92)80008-E)

Total number of authors:
1

Creative Commons License:
Unspecified

General rights

Unless other specific re-use rights are stated the following general rights apply:
Copyright and moral rights for the publications made accessible in the public portal are retained by the authors and/or other copyright owners and it is a condition of accessing publications that users recognise and abide by the legal requirements associated with these rights.

- Users may download and print one copy of any publication from the public portal for the purpose of private study or research.
- You may not further distribute the material or use it for any profit-making activity or commercial gain
- You may freely distribute the URL identifying the publication in the public portal

Read more about Creative commons licenses: <https://creativecommons.org/licenses/>

Take down policy

If you believe that this document breaches copyright please contact us providing details, and we will remove access to the work immediately and investigate your claim.

LUND UNIVERSITY

PO Box 117
221 00 Lund
+46 46-222 00 00

A MODE III CRACK SUBJECTED TO HIGH STRAIN RATES†

P. STÅHLE

Department of Technology, Uppsala University, S-751 21 Uppsala, Sweden

(Received 22 October 1990; in revised form 9 April 1991)

ABSTRACT

THE DISPLACEMENT rate is given for a mode III crack growing in a steady state under dynamic conditions. The material is assumed to be visco-plastic and high strain rates are considered. A regular perturbation expansion is performed. First-order perturbing strains are, with one exception, square root singular near the crack-tip. For overstress exponents less, or equal to 2, a reasonably large region around the crack tip, i.e. $> 10^{-3}$ of the linear extent of the plastic zone, is dominated by the square root singular strain field. For an overstress exponent of $5/2$ the region extends to about 10^{-3} of the plastic zone size, which significantly reduces the possibilities of using the strength of the square root singular field as a fracture parameter. For the overstress exponent 3 the region vanishes.

1. INTRODUCTION

IN MANY situations of fast crack growth in structural steels, the viscosity during plastic straining cannot be ignored [cf. LO (1983) and BRICKSTAD (1983)]. In fact, the viscous behaviour is in some cases so strong that the plastic straining has a limited effect on the stress distribution around the running crack tip. Mode I cases of this kind have been treated by FREUND and HUTCHINSON (1985). They considered the energy rate balance that is necessary for continuous steady-state crack growth. The elastic energy release rate G was balanced essentially by the rate of plastic deformation work and the crack-tip driving force G_{tip} . The method determines G_{tip} and the asymptotic stress and strain field. However, the extent of the region where the asymptotic field dominates remains undetermined.

In this paper, cases of mode III fracture are studied. The following relation [cf. PERZYNA (1963)] between deformation rate \dot{w} and stress is used:

$$\mu \frac{\partial \dot{w}}{\partial x} = \dot{\tau}_{xz} + \dot{\gamma}_0 \tau_t \left(\frac{\tau}{\tau_t} - 1 \right)^n \frac{\tau_{xz}}{\tau} \quad (1)$$

and

$$\mu \frac{\partial \dot{w}}{\partial y} = \dot{\tau}_{yz} + \dot{\gamma}_0 \tau_t \left(\frac{\tau}{\tau_t} - 1 \right)^n \frac{\tau_{yz}}{\tau}, \quad (2)$$

† This paper was prepared during a sabbatical year at the Division of Engineering, Brown University, Providence, RI 02912, U.S.A.

for $\tau \geq \tau_t$, where $\tau = (\tau_{xz}^2 + \tau_{yz}^2)^{1/2}$ is the effective stress, τ_t is the transition stress and μ is the shear modulus. For $\tau < \tau_t$, the material behaves linearly elastically. The material parameters $\dot{\gamma}_0$ and n are referred to as the strain rate sensitivity and the overstress exponent, respectively.

During steady-state crack growth, elastic strains dominate asymptotically close to the crack-tip if $n < 3$. For these cases, it was shown by LO (1983) that the asymptotic solution is the square root singular stress field, which is well known from the theory of linear elasticity. This has far-reaching implications. The most important of these is that a stress intensity factor K_{tip} can, under certain conditions, be defined to describe completely the near-tip state in the way that the conventional dynamic stress intensity factor K_{III} does at small-scale yielding.

FREUND and HUTCHINSON (1985) calculated the plastic strain rates for mode I, using the near-tip field stress distribution. They further showed that this leads to a solution that is valid when the plastic dissipation is an infinitesimal fraction of the total energy release rate. Because of the mathematical simplicity characterizing mode III, treated here, the displacement rate in the entire body can be obtained. Solutions are studied for $n = 1, 2$ and $5/2$ with emphasis on the extent of the region where the square root singular solution dominates. The case $n = 3$ is also compiled, and it is shown that an $r^{-1/2} \log(r)$ singularity develops for the plastic strains. Since this singularity is stronger than the elastic strain singularity, the assumption of small plastic strains will be violated close to the crack tip.

The presence of a near-tip square root singular field allows for simplified analyses, i.e. the process region may be treated as a point. In a real situation, the process region has a finite extent and a necessary condition, allowing for the simplified treatment, is of course that the elastic strains dominate over a region much larger than the process region. This condition is, however, very seldom checked. One reason may be difficulties in determining the extent of the process region. Probably most important, however (to the knowledge of the author), is that there are no available estimates of the region of dominance of the square root singular field.

The present analysis is limited to small speeds m . However, experiments show that speeds exceeding 0.3–0.4 are very seldom reached, e.g. on wide plates of 533B steel (NAUSS *et al.*, 1987). The accuracy here is to the order of m^5 . One might get an indication of the accuracy of the results by noting that $m^6 = 0.004$ for $m = 0.4$. It was further shown for the wide plate experiments that a good portion of the crack growth could be considered to occur at high large strain rates (preferably below room temperatures) (STÄHLE and FREUND, 1989). It is, therefore, believed that the results cover cases of interest for engineering practice. The selected mode of fracture is, however, a severe limitation in the respect that this case seldom occurs in real situations. The reason for selecting mode III is its mathematical simplicity and hopefully the conclusions have some relevance also for mode I cracks.

2. THE PROBLEM

Consider an infinitely large visco-plastic body. A sharp crack is running in the plane $y = 0$ with a speed \dot{a} relative to the body. A frame of reference moving with the crack

is employed, so that the crack edge is situated at $x = y = 0$ (see Fig. 1). The material behaviour is given by (1) and (2) for $\tau \geq \tau_y$, and linear elasticity is assumed for $\tau < \tau_y$. Small strains and deformations are assumed. The boundary tractions are such that the scale of yielding is small, and the stresses far away from the crack tip are given by [cf. ESHELBY (1969)]

$$\tau_{xz} \rightarrow -\frac{K_{III}}{\alpha(2\pi r)^{1/2}} \sin\left(\frac{\theta}{2}\right) \quad \text{and} \quad \tau_{yz} \rightarrow \frac{K_{III}}{(2\pi r)^{1/2}} \cos\left(\frac{\theta}{2}\right) \quad \text{as } r \rightarrow \infty, \quad (3)$$

where K_{III} is the stress intensity factor and r and θ define an elliptic polar coordinate system attached to the crack tip. These coordinates are given as follows:

$$r = (x^2 + \alpha^2 y^2)^{1/2} \quad \text{and} \quad \theta = \tan^{-1}\left(\frac{\alpha y}{x}\right), \quad (4)$$

where

$$\alpha = (1 - m^2)^{1/2} \quad \text{and} \quad m = \frac{\dot{a}}{c_s}. \quad (5)$$

The only significant elastic wave speed for mode III is the shear wave speed c_s , which is defined by

$$c_s = \left(\frac{\mu}{\rho}\right)^{1/2}, \quad (6)$$

where ρ is the mass density. It was shown by ACHENBACH and BAZANT (1975) that the near-tip field for a crack running in a linearly elastic material is in a steady state. Here it is assumed that this also holds for a sufficiently small scale of yielding. The steady state implies that

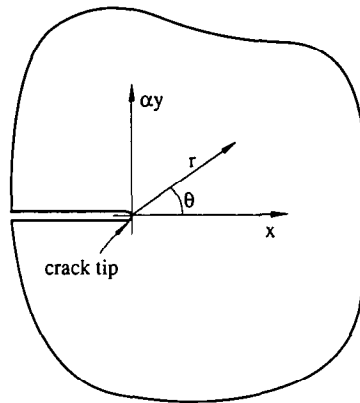


FIG. 1. Coordinate systems attached to the moving crack tip.

$$(\dot{}) \equiv -\dot{a} \frac{\partial}{\partial x}, \quad (7)$$

where $(\dot{})$ denotes differentiation of any state parameter with respect to time. The equation of motion is

$$\frac{\partial \tau_{xz}}{\partial x} + \frac{\partial \tau_{yz}}{\partial y} = \rho \ddot{w}. \quad (8)$$

By differentiating (8) with respect to time and then reducing the time derivatives of the displacement rate by applying (7),

$$\frac{\partial \dot{\tau}_{xz}}{\partial x} + \frac{\partial \dot{\tau}_{yz}}{\partial y} = \mu m^2 \frac{\partial^2 \dot{w}}{\partial x^2} \quad (9)$$

is obtained. For convenience the following fluidity parameter,

$$\lambda = \frac{\dot{\gamma}_0 K_{III}^2}{\dot{a} \tau_i \mu}, \quad (10)$$

is introduced. Insertion of (1), (2) and (10) into (9) leads to

$$\frac{\partial^2 \dot{w}}{\partial x^2} + \frac{\partial^2 \dot{w}}{\alpha^2 \partial y^2} = \frac{\lambda \dot{a} \tau_i^2}{\alpha^2 K_{III}^2} \left\{ \frac{\partial}{\partial x} \left[\left(\frac{\tau}{\tau_i} - 1 \right)^n \frac{\tau_{xz}}{\tau} \right] + \frac{\partial}{\partial y} \left[\left(\frac{\tau}{\tau_i} - 1 \right)^n \frac{\tau_{yz}}{\tau} \right] \right\}, \quad (11)$$

for $\tau \geq \tau_i$.

If nothing else is explicitly declared, the continued calculations are confined to the plastic region where $\tau \geq \tau_i$. Further, the fluidity is assumed to be small, i.e. it is assumed that $\lambda \ll 1$.

A regular perturbation expansion is suggested. It is thus assumed that the solution to (11) may be expanded as

$$\dot{w} = \dot{w}_0 + \lambda \dot{w}_1 + O(\lambda)^2 \dot{w}_2, \quad (12)$$

$$\tau_{xz} = \tau_{xz0} + \lambda \tau_{xz1} + O(\lambda)^2 \tau_{xz2} \quad (13)$$

and

$$\tau_{yz} = \tau_{yz0} + \lambda \tau_{yz1} + O(\lambda)^2 \tau_{yz2}. \quad (14)$$

Third-order terms are neglected, i.e. those of the order of λ^2 . A perturbation expansion is expected to work for $n < 3$ since this limit guarantees that the singularity at $r = 0$ of the perturbing terms, $\dot{w}_1, \dot{w}_2, \dots$ (with $\dot{w} = \sum \lambda^i \dot{w}_i$) is weaker than the zeroth-order term, \dot{w}_0 . Assume just for a moment that $\dot{w}_i = O(r^{s_i})$ as $r \rightarrow 0$. Let it be required that

$$s_{i+1} > s_i \quad \text{for } i = 0, 1, 2, \dots \quad (15)$$

According to (1) and (2), τ_{xzi} and τ_{yzi} are of the order of r^{s_i} as $r \rightarrow 0$. The right-hand side of (11) is then of the order of r^{ns_i-1} and accordingly

$$\dot{w}_{i+1} r^{-2} = O(r)^{ns_i-1} \quad \text{as } r \rightarrow 0. \quad (16)$$

It follows from (15) and (16) that

$$ns_i - 1 = s_{i+1} - 2 > s_i - 2. \quad (17)$$

It is further necessary that the energy release rate at the crack tip is finite, which implies that $s_0 = -1/2$. After insertion into (17)

$$n < 3 \quad (18)$$

is obtained, which imposes a limit for the present analysis.

Equation (11) leaves the following two requirements:

$$\alpha^2 \frac{\partial^2 \dot{w}_0}{\partial x^2} + \frac{\partial^2 \dot{w}_0}{\partial y^2} = 0 \quad (19)$$

and

$$\frac{\partial^2 \dot{w}_1}{\partial x^2} + \frac{\partial^2 \dot{w}_1}{\alpha^2 \partial y^2} = \frac{\dot{\alpha} \tau_i^2}{\alpha^2 K_{III}^2} \frac{\partial}{\partial x} \left[\left(\frac{\tau_0}{\tau_i} - 1 \right)^n \frac{\tau_{xz0}}{\tau_0} \right] + \frac{\partial}{\partial y} \left[\left(\frac{\tau_0}{\tau_i} - 1 \right)^n \frac{\tau_{yz0}}{\tau_0} \right], \quad (20)$$

where $\tau_0 = (\tau_{xz0}^2 + \tau_{yz0}^2)^{1/2}$. Obviously \dot{w}_0 is the linearly elastic solution

$$\dot{w}_0 = \frac{\dot{\alpha} K_{III}}{\alpha \mu (2\pi r)^{1/2}} \sin\left(\frac{\theta}{2}\right). \quad (21)$$

The dynamic stress intensity factor K_{III} is related to the elastic energy release rate G as

$$G = \frac{K_{III}^2}{\alpha \mu}. \quad (22)$$

The shapes of the plastic zones at different crack-tip speeds are shown in Appendix A. As observed, the zone size expands indefinitely as the shear wave speed is approached, i.e. as $\alpha \rightarrow 0$.

Equation (20) will be solved in $\tau \geq \tau_i$ and in $\tau < \tau_i$ by means of Fourier series. The solution for the elastic material and the solution for the visco-plastic material have to be matched across the elastic plastic boundary, $\tau = \tau_i$. Therefore, a simpler description of the elastic plastic boundary than (A6) is desired. That can be obtained through application of a hodograph-related transform [cf. FREUND and DOUGLAS (1968) or COURANT and HILBERT (1953)]. The following coordinates are used:

$$t_x = \frac{\tau_{xz0}}{\tau_i} = -\frac{K_{III}}{\alpha \tau_i (2\pi r)^{1/2}} \sin\left(\frac{\theta}{2}\right) \quad (23)$$

and

$$t_y = \frac{\tau_{yz0}}{\tau_i} = \frac{K_{III}}{\tau_i (2\pi r)^{1/2}} \cos\left(\frac{\theta}{2}\right). \quad (24)$$

A polar coordinate system, t and φ , is attached to the origin of the t_x - t_y plane. Define

$$t = (t_x^2 + t_y^2)^{1/2} \quad \text{and} \quad \varphi = \tan^{-1} \left(\frac{t_x}{t_y} \right). \quad (25)$$

The elastic plastic boundary at vanishing plastic strains is now given by $t = 1$ and $|\varphi| \leq \pi/2$. The boundaries in the t_x - t_y plane are shown in Fig. 2(a) and (b). The segments in Fig. 2(a) correspond to the respective primed segments in Fig. 2(b). Note that w is anti-symmetric with respect to $\varphi = 0$. It is further obvious that $\partial \dot{w} / \partial \varphi = 0$ at $\varphi = \pi/2$, since here $\theta = \pi$ and thus $\partial \dot{w} / \partial \varphi$ is proportional to $\partial \dot{w} / \partial y$, which in its turn is proportional to \dot{t}_y , and along the stress-free crack surface $\dot{t}_y = 0$. Thus $\partial \dot{w} / \partial \varphi = 0$ along the segments Γ'_A and Γ'_B and $w = 0$ along Γ'_F and Γ'_E .

On the left-hand side of (20), here denoted LH the chain rule is applied:

$$\begin{aligned} \text{LH} = \frac{\partial^2 \dot{w}_1}{\partial x^2} + \frac{\partial^2 \dot{w}_1}{\alpha^2 \partial y^2} &= \frac{\partial^2 \dot{w}_1}{\partial r^2} + \frac{\partial \dot{w}_1}{r \partial r} + \frac{\partial^2 \dot{w}_1}{r^2 \partial \theta^2} = \left[\left(\frac{\partial t}{\partial r} \right)^2 + \left(\frac{\partial t}{r \partial \theta} \right)^2 \right] \frac{\partial^2 \dot{w}_1}{\partial t^2} \\ &+ \left(\frac{\partial^2 t}{\partial r^2} + \frac{\partial t}{r \partial r} + \frac{\partial^2 t}{r^2 \partial \theta^2} \right) \frac{\partial \dot{w}_1}{\partial t} + 2 \frac{\partial t}{r \partial \theta} \frac{\partial \varphi}{r \partial \theta} \frac{\partial^2 \dot{w}_1}{\partial t \partial \varphi} + \frac{\partial^2 \varphi}{r^2 \partial \theta^2} \frac{\partial \dot{w}_1}{\partial \varphi} + \left(\frac{\partial \varphi}{r \partial \theta} \right)^2 \frac{\partial^2 \dot{w}_1}{\partial \varphi^2}. \end{aligned} \quad (26)$$

Note that $\partial \varphi / \partial r = 0$. The following substitutions are made:

$$\left. \begin{aligned} \frac{\partial t}{\partial r} &= -\frac{t}{2} (t^2 - m^2 t_x^2) \left(\frac{\tau_t}{K_{III}} \right)^2, & \frac{\partial^2 t}{\partial r^2} &= \frac{3t}{4} (t^2 - m^2 t_x^2)^2 \left(\frac{\tau_t}{K_{III}} \right)^4, \\ \frac{\partial t}{\partial \theta} &= -\frac{m^2 t_x t_y}{2\alpha t}, & \frac{\partial^2 t}{\partial \theta^2} &= \frac{m^2 [t^2 (t^2 - 2t_x^2) + m^2 t_x^4]}{4\alpha^2 t^3}, \\ \frac{\partial \varphi}{\partial \theta} &= -\frac{t^2 - m^2 t_x^2}{2\alpha t^2} \quad \text{and} \quad \frac{\partial^2 \varphi}{\partial \theta^2} &= -\frac{m^2 t_x t_y (t^2 - m^2 t_x^2)}{2\alpha^2 t^4}. \end{aligned} \right\} \quad (27)$$

LH is now transformed to

$$\begin{aligned} \text{LH} = \frac{(t^2 - m^2 t_x^2)^3 \tau_t^4}{4\alpha^2 t^2 K_{III}^4} &\left[(t^2 - m^2 t_x^2) \frac{\partial^2 \dot{w}_1}{\partial t^2} + 2m^2 t_x t_y \left(\frac{\partial}{\partial t} - \frac{1}{t} \right) \frac{\partial \dot{w}_1}{t \partial \varphi} \right. \\ &\left. + (t^2 - m^2 t_x^2) \left(\frac{\partial \dot{w}_1}{t \partial t} + \frac{\partial^2 \dot{w}_1}{t^2 \partial \varphi^2} \right) \right]. \end{aligned} \quad (28)$$

After inserting (23) and (24) into the right-hand side of (20), RH,

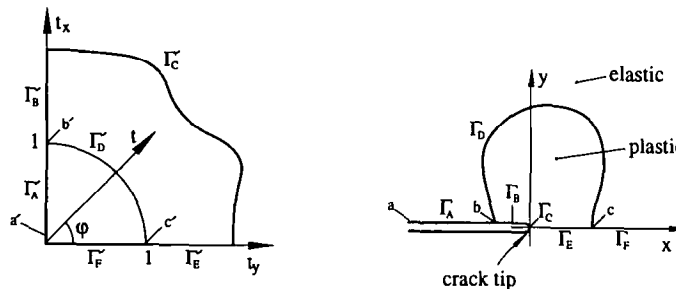


FIG. 2. Boundaries in the t_x - t_y plane. The segments Γ'_A - Γ'_F in (a) correspond to segments Γ_A - Γ_F in (b).

$$\text{RH} = \frac{\dot{a}\tau_t^2}{\alpha^2 K_{\text{III}}^2} \left\{ \frac{(t-1)^n}{t} \left(\frac{\partial t_x}{\partial x} + \frac{\partial t_y}{\partial y} \right) + \frac{\partial}{\partial t} \left[\frac{(t-1)^n}{t} \right] \left(t_x \frac{\partial t}{\partial x} + t_y \frac{\partial t}{\partial y} \right) \right\} \quad (29)$$

is obtained.

The following relations become useful:

$$\left. \begin{aligned} \frac{\partial t_x}{\partial x} &= -\frac{\partial t_y}{\alpha^2 \partial y} = \frac{t_x}{2} (\alpha^2 t_x^2 - 3t_y^2) \left(\frac{\tau_t}{K_{\text{III}}} \right)^2, \\ \frac{\partial t_y}{\partial x} &= \frac{\partial t_x}{\partial y} = \frac{t_y}{2} (3\alpha^2 t_x^2 - t_y^2) \left(\frac{\tau_t}{K_{\text{III}}} \right)^2, \\ \frac{\partial t}{\partial t_x} &= \frac{t_x}{t} \quad \text{and} \quad \frac{\partial t}{\partial t_y} = \frac{t_y}{t}. \end{aligned} \right\} \quad (30)$$

After substitution of these expressions into (29), RH appears as follows:

$$\text{RH} = \frac{\dot{a}\tau_t^4 t_x (t-1)^n}{2\alpha^2 K_{\text{III}}^4 t^3} \left\{ \frac{[(n-1)t+1]}{t-1} [t^4 - m^2 t^2 (t^2 + 2t_y^2) - m^4 t_y^2 t_y^2] + m^2 t^2 (t^2 - 4t_y^2 - m^2 t_y^2) \right\}. \quad (31)$$

Putting again LH = RH and using the definitions (25), (20) is now written as

$$\begin{aligned} [1 - m^2 \sin^2(\varphi)] t^2 \Delta_t \dot{w}_1 + m^2 \left[\sin(2\varphi) \left(\frac{t}{\partial t} - 1 \right) \frac{\partial \dot{w}_1}{\partial \varphi} - \cos(2\varphi) t^3 \frac{\partial^2 \dot{w}_1}{\partial t^2} \right] \\ = \frac{2\dot{a}(t-1)^{n-1}}{t^2 [1 - m^2 \sin^2(\varphi)]^3} \{ [(n-1)t+1 - 3m^2 nt] \sin(\varphi) \\ + m^2 [2(n+1)t - 2 - m^2 nt] \sin^3(\varphi) + m^4 [(n-1)t+1] \sin^5(\varphi) \}, \quad (32) \end{aligned}$$

where

$$\Delta_t \equiv \frac{\partial^2}{\partial t^2} + \frac{\partial}{t \partial t} + \frac{\partial^2}{t^2 \partial \varphi^2}.$$

The boundary conditions ($\partial \dot{w}_1 / \partial \varphi = 0$ along $t_x = 0$ and $\dot{w}_1 = 0$ along $t_y = 0$) suggest that the solution can be expanded in the following Fourier series:

$$\dot{w}_1 = \dot{a} \sum_{q=1,3,5}^{\infty} f_q(t) \sin(q\varphi). \quad (33)$$

Insertion into the left-hand side of (32) gives

$$\dot{a} \sum_{q=1,3,5}^{\infty} \left(\left(1 - \frac{m^2}{2} \right) (t^2 f_q'' + t f_q' - q^2 f_q) \sin(q\varphi) - \frac{m^2}{4} \{ [t^2 f_q'' + (2q-1)t f_q' + q(q-2)f_q] \sin[(q-2)\varphi] + [t^2 f_q'' - (2q+1)t f_q' + q(q+2)f_q] \sin[(q+2)\varphi] \} \right). \quad (34)$$

After changing the order of summation one may write

$$\dot{a} \sum_{q=1,3,5}^{\infty} \left\{ \left(1 - \frac{m^2}{2} \right) (t^2 f_q'' + t f_q' - q^2 f_q) - \frac{m^2}{4} [t^2 f_{q-2}'' - (2q-3)t f_{q-2}' + q(q-2)f_{q-2} + t^2 f_{q+2}'' + (2q+3)t f_{q+2}' + q(q+2)f_{q+2}] \right\} \sin(q\varphi). \quad (35)$$

Turning now to the right-hand side of (32), after expanding in m and by changing to trigonometric expressions for multiple angles,

$$\frac{2\dot{a}(t-1)^{n-1}}{t^2} \left\{ \left(1 + \frac{3m^2}{4} + \frac{5m^4}{8} \right) [(n-1)t+1] \sin(\varphi) - \left(\frac{m^2}{4} + \frac{5m^4}{16} \right) [(5n-1)t+1] \sin(3\varphi) + \frac{m^4}{16} [(13n-1)t+1] \sin(5\varphi) \right\} + O(m)^6 \quad (36)$$

is obtained.

It is useful to notice that the character of (32) leads to $f_q = O(f_{q-2} m^2)$. The observation that f_1 is of the order of m^0 as $m \rightarrow 0$ implies that $f_q = O(m)^{q-1}$. Consequently, since truncation is desired for terms of order m^6 , one may neglect f_q for $q \geq 7$. Inserting (35) and (36) back into (32) gives three equations to solve:

$$\begin{aligned} \left(1 - \frac{m^2}{4} \right) (t^2 f_1'' + t f_1' - f_1) - \frac{m^2}{4} (t^2 f_3'' + 5t f_3' + 3f_3) \\ = \frac{2(t-1)^{n-1}}{t^2} \left(1 - \frac{m^2}{4} - \frac{m^4}{8} \right) [(n-1)t+1] + O(m)^6, \quad (37) \end{aligned}$$

$$\begin{aligned} \left(1 - \frac{m^2}{2} \right) (t^2 f_3'' + t f_3' - 9f_3) - \frac{m^2}{4} (t^2 f_1'' - 3t f_1' + 3f_1 + 2t^2 f_5'' + 18t f_5' + 30f_5) \\ = - \frac{(t-1)^{n-1}}{2t^6} \left(1 + \frac{m^2}{4} \right) [(5n-1)t+1] + O(m)^6 \quad (38) \end{aligned}$$

and

$$\begin{aligned} \left(1 - \frac{m^2}{2} \right) (t^2 f_5'' + t f_5' - 25f_5) - \frac{m^2}{4} (t^2 f_3'' - 7t f_3' + 15f_3) \\ = \frac{(t-1)^{n-1}}{8t^6} [(13n-1)t+1] + O(m)^6. \quad (39) \end{aligned}$$

A matching of homogeneous solutions for $\tau < \tau_i$ with homogeneous and particular solutions for $\tau > \tau_i$ has to be done. The condition used is that continuous velocities \dot{w} and accelerations \ddot{w} are required everywhere and thus also across the boundary at $\tau = \tau_i$ [cf. HILL (1961)]. The plastic deformation affects the plastic zone shape, i.e. the elastic plastic boundary is shifted from the curve $t = 1$ by a quantity of the order of λ [cf. (A6) in Appendix A]. Let w_+ denote the solution in the plastic zone and w_- the solution outside the plastic zone.

The elastic boundary is situated at $t = 1 + \varepsilon$, where $\varepsilon = O(\lambda)$. The continuity conditions are

$$[\dot{w}_+ - \dot{w}_-]_{t=1+\varepsilon} = 0 \quad (40)$$

and

$$\left[\frac{\partial \dot{w}_+}{\partial t} - \frac{\partial \dot{w}_-}{\partial t} \right]_{t=1+\varepsilon} = 0. \quad (41)$$

This implies that

$$[\dot{w}_+ - \dot{w}_-]_{t=1} + \varepsilon \left[\frac{\partial \dot{w}_+}{\partial t} - \frac{\partial \dot{w}_-}{\partial t} \right]_{t=1} + O(\lambda)^2 = 0 \quad (42)$$

and

$$\left[\frac{\partial \dot{w}_+}{\partial t} - \frac{\partial \dot{w}_-}{\partial t} \right]_{t=1} + \varepsilon \left[\frac{\partial^2 \dot{w}_+}{\partial t^2} - \frac{\partial^2 \dot{w}_-}{\partial t^2} \right]_{t=1} + O(\lambda)^2 = 0. \quad (43)$$

It is assumed that w_+ or w_- is analytically continued across the elastic plastic boundary. Generally $\partial \dot{w}^2 / \partial t^2$ is discontinuous across the elastic plastic boundary. However, the second derivative of the zeroth-order solution, $\partial \dot{w}_0^2 / \partial t^2$, is continuous since the viscosity effects only enter to the order of λ . Continuity is in the present analysis only required to the order of the accuracy of \dot{w} , i.e. λ . This means that the continuity conditions (40) and (41) may be written as

$$[\dot{w}_+ - \dot{w}_-]_{t=1} = O(\lambda)^2 \quad \text{and} \quad \left[\frac{\partial \dot{w}_+}{\partial t} - \frac{\partial \dot{w}_-}{\partial t} \right]_{t=1} = O(\lambda)^2. \quad (44)$$

The elastic plastic boundary is shifted a distance which is of the order of λ . Even so, as (44) state, the perturbed shape of the plastic zone will make its influence on \dot{w} felt only to the order of λ^2 .

Solutions truncated for $O(m)^6$ can be found in Appendix B. Here, only the quasi-static solutions are given. The length parameter is defined as

$$R = \frac{K_{III}^2}{2\pi\tau_i^2}, \quad (45)$$

which to the order of λ equals the linear extent of the plastic zone straight ahead of the crack tip. After putting $\hat{r} = r/R$ one obtains for $n = 1$

$$\dot{w} = \left\{ \left(\frac{\dot{a}}{\dot{\gamma}_0 R} - \frac{1}{3} \right) \hat{r}^{-1/2} + \hat{r}^{1/2} - \frac{2}{3} \hat{r} \right\} \Gamma + O(m)^2, \quad (46)$$

for $n = 2$

$$\dot{w} = \left\{ \left(\frac{\dot{a}}{\dot{\gamma}_0 R} - \frac{2}{3} \right) \hat{r}^{-1/2} + 2 - 2\hat{r}^{1/2} + \frac{2}{3} \hat{r} \right\} \Gamma + O(m)^2 \quad (47)$$

and for $n = 5/2$

$$\dot{w} = \left\{ \left[\frac{\dot{a}}{\dot{\gamma}_0 R} - \frac{5 \tan^{-1}(z)}{4} \right] \hat{r}^{-1/2} + \left(\frac{11}{4} - \frac{13}{6} \hat{r}^{1/2} + \frac{2}{3} \hat{r} \right) z \right\} \Gamma + O(m)^2, \quad (48)$$

where

$$z = (\hat{r}^{-1/2} - 1)^{1/2}.$$

For $n = 3$

$$\dot{w} = \left\{ \left[\frac{\dot{a}}{\dot{\gamma}_0 R} + \frac{11}{3} + \log(\hat{r}) \right] \hat{r}^{-1/2} - 6 + 3\hat{r}^{1/2} - \frac{2}{3} \hat{r} \right\} \Gamma + O(m)^2. \quad (49)$$

The function Γ is given by

$$\Gamma = \frac{R \dot{\gamma}_0 \tau_t}{\mu} \sin\left(\frac{\theta}{2}\right). \quad (50)$$

Solutions (46)–(48) are valid only in the plastic zone, i.e. for $\hat{r} \leq 1$. The solution for $n = 3$ [(49)] violates the inequality (15). Thus the strains cannot be expected to be elastic close to the crack tip. A weaker singularity will develop and the result for $n = 3$ is therefore not of any further interest in the present analysis.

It is the case that

$$\dot{w} = \frac{\dot{a} \tau_t}{\mu \hat{r}^{1/2}} \sin\left(\frac{\theta}{2}\right) + O(m)^2, \quad (51)$$

outside the plastic zone, i.e. for $\hat{r} > 1$. This means that the effects of fluidity in the quasi-static limit vanish at the elastic plastic boundary. Somewhat surprisingly, this holds independent of n . However, that is not the case for dynamic cracks as can be seen in (B10)–(B12) in Appendix B.

3. RESULTS AND DISCUSSION

The question of defining the extent of the region where the square root singular terms dominate can, of course, be given many answers. The present study is compiled under the assumption of small deviations from the elastic stress and strain distribution as a whole. Note that the deviations consist of terms proportional to the strain rate sensitivity $\dot{\gamma}_0$ [see (46)–(48)]. Of these terms the most dominant is of the order of $r^{-1/2}$

for overstress exponents $n = 1, 2$ and $5/2$. The plastic deformation work per unit of crack extension is given by the amplitude of this term, and the result can be compared with the result found through calculation of an energy balance (see Appendix C).

Here, a parameter \tilde{K}_{III} is defined as

$$\tilde{K}_{III}(r) = \frac{\mu(2\pi r)^{1/2}\dot{w}}{\dot{a} \sin\left(\frac{\theta}{2}\right)} \tag{52}$$

At a large distance from the crack tip \tilde{K}_{III} approaches the elastic stress intensity factor K_{III} , i.e.

$$\lim_{r \rightarrow \infty} \tilde{K}_{III}(r) = K_{III} \tag{53}$$

As the crack tip is approached, it is found that

$$\lim_{r \rightarrow 0} \tilde{K}_{III}(r) = K_{up} = \left[1 - \delta g(m) \frac{(\mu\rho)^{1/2} G_{up}}{6\tau_c^2} \right] K_{III} \tag{54}$$

where $g(m)$ and the factor δ can be obtained from (B7), (B8) and (47). Equation (54) is accurate to the order of λ . In Appendix C the exact result for the limit as $r \rightarrow 0$ is found by applying the theory of FREUND and HUTCHINSON (1985). The speed function $g(m)$ is found to be independent of n and the result according to (C5) is

$$g(m) = \frac{8 - 8m^2 + 3m^4}{8m(1 - m^2)^{3/2}} = \frac{1}{m} + \frac{m}{2} + \frac{3m^3}{4} + O(m)^5 \tag{55}$$

The magnitude is chosen so that $m \times g(m) \rightarrow 1$. The parameter δ is determined to be as given in Table 1. An approximation of $\delta \times g(m)$ can be obtained from (B7). By putting δ according to Table 1, the following are obtained for $n = 1, 2$ and $5/2$:

$$g(m) = \frac{(1 - m^2)}{m} \left[1 + \frac{3}{2}m^2 + \frac{9}{4}m^4 + O(m)^6 \right] \tag{56}$$

which coincides to the order of m^5 with the result (55). Figure 3 shows $g(m)$ for $0 < m < 1$. It is observed that $g(m)$ has a minimum in the interval. Through differentiation of (55) with respect to m the following solution is obtained:

TABLE 1. Factor δ for different overstress exponents n

n	δ
1	$1(2\pi)$
2	$1/\pi$
5/2	15/16
3	∞

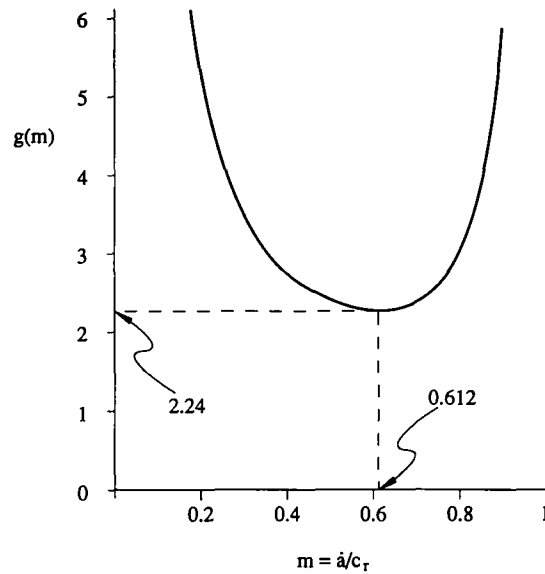


FIG. 3. Function $g(m)$. The minimum 2.24 of g is found at $m = 0.612$.

$$m_{\min} = \left(\frac{12 - 2 \times 22^{1/2}}{7} \right)^{1/2} \approx 0.6117. \quad (57)$$

At this speed a crack can be driven by the least possible energy release rate G , assuming that the crack-tip driving force G_{tip} is constant. Insertion of $m = m_{\min}$ into (55) gives $g(m_{\min}) \approx 2.2399$. In the quasi-static limit $m \times g(m) \rightarrow 1$.

The primary scope of this paper is to estimate the extent of the region where the square root singular solution dominates. Since K_{tip} fully determines the asymptotic behaviour, it is of interest to study how far away from the crack tip K_{tip} actually provides a good approximation of \tilde{K}_{III} .

Figure 4 shows the relative difference between \tilde{K}_{III} and K_{tip} in the form of the following measure:

$$f = \frac{\tilde{K}_{\text{III}}(r) - K_{\text{tip}}}{K_{\text{tip}} - K_{\text{III}}}. \quad (58)$$

As observed, the region of K_{tip} dominance decreases with increasing values of n . Use K_{tip} as an estimate of \tilde{K}_{III} , with an accuracy depending on r . Assume further that, for instance, 90% of the shielding effect that the plastic straining has on the stress intensity factor has to be captured. Then K_{tip} may be approximated by \tilde{K}_{III} only closer to the crack tip than about 0.03 of the distance R to the elastic plastic boundary straight ahead of the crack tip, for $n = 1$. The corresponding distance for $n = 2$ is about $0.001R$ and for $n = 5/2$ the distance is about $10^{-5}R$. This is a fairly small distance and the size of the process region cannot be expected to be much smaller than that. It is proposed that $n = 2$ is a limiting case which leaves us with the conclusion that

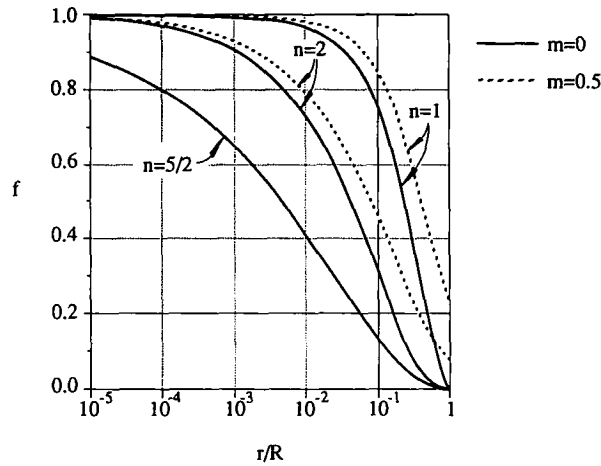


FIG. 4. Variation of apparent stress intensity factor \tilde{K}_{III} vs distance from the crack tip for $\dot{a}/c \rightarrow 0$ and $\dot{a} = 0.5c_1$.

the approximation of K_{tip} with \tilde{K}_{III} cannot safely be used for materials with $n > 2$. At higher speeds the result improves somewhat but not enough to essentially change our conclusion.

The region where the asymptotic (square root singular) field for the plastic effects describes the actual plastic effects on the displacement rate, $\dot{w} - \dot{w}_0$, depends, of course, on what the desired level of accuracy is. The accuracy is here taken to be $1 - f$, where f is given by (58). In the quasi-static case, this region is a circle. In the dynamic case

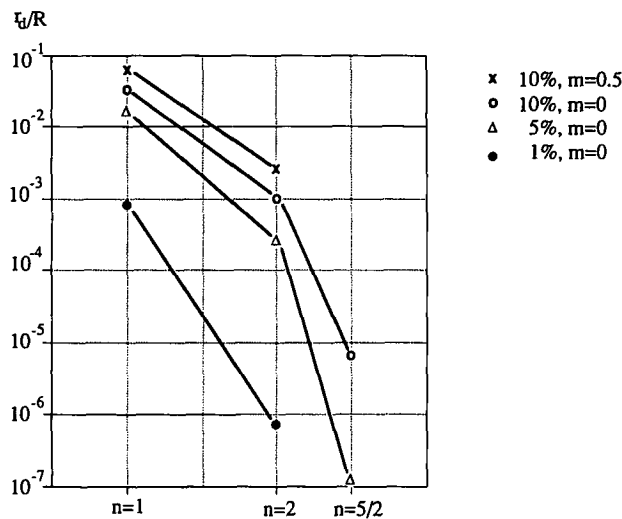


FIG. 5. Extent straight ahead of the crack tip of the region of dominance for the asymptotic field for different materials and levels of accuracy. The accuracy is given by $1 - f$. The region is nearly circular for crack-tip speeds of interest, say $m < 0.5$.

the deviation from the circular shape is insignificant, at least for speeds of practical relevance, for say $m < 0.5$. The radius of this region in the quasi-static case and the extent straight ahead of the crack tip in the dynamic case is shown in Fig. 5, for different levels of accuracy. It is noted that, if a higher accuracy is desired, e.g. 1%, then a reasonably large region of dominance for the asymptotic field cannot be found for materials with $n > 1$.

For $n = 3$ the model develops an $r^{-1/2} \log(r)$ strain singularity. This is stronger than the square root singular field, implying that the apparent stress intensity factor \tilde{K}_{III} is likely to decrease towards zero as the crack tip is approached. When the plastic strains become of the order of the elastic strains, the limit for the present theory will be exceeded. The analysis is uncertain in this case since the effect on the solution due to the different conditions at the crack tip is unknown. Thus, the character of the asymptotic field for $n = 3$ is not determined in the present analysis.

ACKNOWLEDGEMENTS

Support during the author's visit to Brown University, received from the Gyllenstiern Krappereup Foundation and the Office of Naval Research through contract N00014-87-K-0481, is gratefully acknowledged.

REFERENCES

- | | | |
|---|------|--|
| ACHENBACH, J. D. and
BAZANT, Z. P. | 1975 | <i>J. appl. Mech.</i> 42 , 183. |
| BRICKSTAD, B. | 1983 | <i>J. Mech. Phys. Solids</i> 31 , 307. |
| COURANT, R. and HILBERT, D. | 1953 | <i>Methods of Mathematical Physics</i> . Interscience, New York. |
| ESHELBY, J. D. | 1969 | <i>J. Mech. Phys. Solids</i> 17 , 177. |
| FREUND, L. B. and
DOUGLAS, A. S. | 1982 | <i>J. Mech. Phys. Solids</i> 30 , 59. |
| FREUND, L. B. and
HUTCHINSON, J. | 1985 | <i>J. Mech. Phys. Solids</i> 33 , 169. |
| HILL, R. | 1961 | <i>J. Mech. Phys. Solids</i> 10 , 1. |
| LO, K. K. | 1983 | <i>J. Mech. Phys. Solids</i> 31 , 287. |
| NAUSS, D. J., NANSTAD, R. K.,
BASS, B. R., MERKLE, J. G.,
PUGH, C. E., CORWIN, W. R.
and ROBINSON, G. C. | 1987 | Crack-arrest behaviour in SEN wide plates of quenched and tempered A 533 grade B steel under nonisothermal conditions. NUREG/CR 4930 ORNL-6388, Oakridge Laboratories. |
| PERZYNA, P. | 1963 | <i>Q. appl. Math.</i> 20 , 321. |
| STÄHLE, P. and FREUND, L. B. | 1990 | Brown University report, N00014-87-K0481. |

APPENDIX A: ELASTIC PLASTIC BOUNDARY AT VANISHING PLASTIC STRAINS

The elastic plastic boundary, given by x_p and y_p is obtained by putting $\tau = \tau_r$. It is found after using (4) that

$$x_p = R_p(\theta) \cos(\theta) \quad \text{and} \quad y_p = \alpha^{-1} R_p(\theta) \sin(\theta), \quad (\text{A1})$$

where

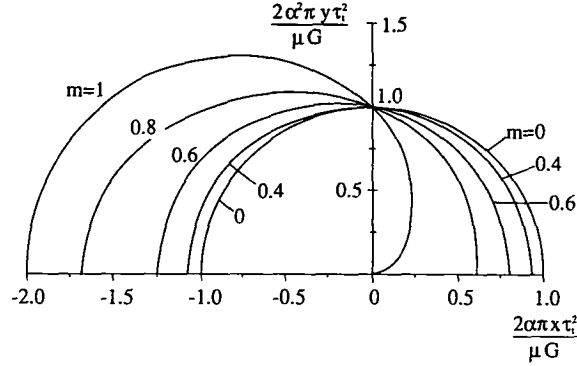


FIG. A1. Elastic plastic boundary at vanishing plastic strains and different crack-tip speeds. The limiting case $\dot{a} \rightarrow c$, is also included.

$$R_p(\theta) = R_{p0}(\theta) + \rho_p(\theta) \quad \text{and} \quad R_{p0}(\theta) = \lim_{\lambda \rightarrow 0} R_p(\theta). \quad (\text{A2})$$

The effective stress τ is given by (13) and (14). One may write

$$\tau(r) = \tau_0(r) + \lambda \tau_1(r) + O(\lambda)^2. \quad (\text{A3})$$

It is assumed that $\rho_p \ll R_{p0}$. After differentiation and insertion of (A2) into (A3)

$$\tau_r = \tau(R_p) = \tau_0(R_{p0}) + \rho_p \left[\frac{\partial \tau_0}{\partial r} \right]_{r=R_{p0}} + \lambda \tau_1(R_{p0}) + O(\lambda)^2 \quad (\text{A4})$$

is obtained, but $\tau_0(R_{p0}) = \tau_r$ and thus

$$\rho_p = -\lambda \tau_1(R_{p0}) / \left[\frac{\partial \tau_0}{\partial r} \right]_{r=R_{p0}} + O(\lambda)^2. \quad (\text{A5})$$

The shape is to the zeroth order of λ obtained by putting $\tau_0 = \tau_r$:

$$R_p(\theta) = \frac{\mu G}{2\pi\alpha\tau_i^2} \left[1 + m^2 \cos^2 \left(\frac{\theta}{2} \right) \right] + O(\lambda) \quad \text{for} \quad -\pi \leq \theta \leq \pi. \quad (\text{A6})$$

Note that $R_p(\theta)$ is the distance from the crack-tip in the elliptic polar coordinate system (4). Figure A1 shows the elastic plastic boundary for a few different values of m for a constant K_{III} and for a constant G . The limiting shape assumed when the crack-tip speed approaches the shear wave speed is included. The normalized coordinate axes indicate how the plastic zone extends indefinitely as $\alpha \rightarrow 0$.

APPENDIX B: SOLUTIONS TRUNCATED FOR $O(m)^6$

The displacement rate is composed of one particular solution, w_p , to (35)–(37) and the solutions, w_h , to the corresponding homogeneous equations. A homogeneous solution to (35)–(37) is given by

$$\begin{aligned} w_h = & A_4 t^{-5} [4 + 3m^2 + 2m^4] \sin(5\varphi) + A_3 t^{-3} [(16 + 20m^2 + 21m^4) \sin(3\varphi) \\ & - (12m^2 + 21m^4) \sin(5\varphi)] + A_2 t^{-1} [(16 + 12m^2 + 10m^4) \sin(\varphi) \\ & - (4m^2 + 5m^4) \sin(3\varphi) + m^4 \sin(5\varphi) + A_1 t \sin(\varphi) + B_1 t^3 [3m^2 \sin(\varphi) + (4 - m^2) \sin(3\varphi)] \\ & + B_2 t^5 [10m^4 \sin(\varphi) + (20m^2 - 5m^4) \sin(3\varphi) + (16 - 12m^2 + m^4) \sin(5\varphi)], \end{aligned} \quad (\text{B1})$$

where A_1, A_4, B_1 and B_2 are undetermined constants. A reasonable requirement is that the effects of crack-tip plasticity vanish on large distances from the crack tip, i.e. $\dot{w} \rightarrow \dot{w}_0$ as $t \rightarrow 0$. This implies that $\dot{w} \rightarrow O(t)$ as $t \rightarrow 0$. Thus, it is obvious that $A_2 = A_3 = A_4 = 0$ in the elastic region and further

$$A_1 = -\frac{\dot{\sigma}_t}{\mu} \quad \text{in } t > 0, \quad \text{i.e. in } r > R_p(0). \quad (\text{B2})$$

It is further noted that B_1 and B_2 are zero in the plastic region since here $\dot{w} = O(t)$ as $t \rightarrow \infty$. It is found that A_1 is the only constant that may be non-zero in the entire plane. It should, however, be remembered that A_1 as well as the other constants (A_2, B_2) may suffer a jump across the elastic plastic boundary.

For $t \geq 1$ the following particular solutions to (35)–(37) are found:

$$\begin{aligned} \dot{w}_p = -\lambda \dot{a} \left\{ \left(1 + m^2 + \frac{37m^4}{40} \right) \frac{2}{3t^2} \sin(\varphi) + \left[1 + \frac{7m^2}{4} - \left(8 + \frac{23m^2}{2} \right) \frac{1}{5t} \right] \frac{m^2}{4t} \sin(3\varphi) \right. \\ \left. + (9 - 7t) \frac{m^4}{56} \sin(5\varphi) \right\} + O(m)^6 \quad (\text{B3}) \end{aligned}$$

for $n = 1$,

$$\begin{aligned} \dot{w}_p = -\lambda \dot{a} \left[2 + 2m^2 + \frac{9m^4}{4} + \left(1 + m^2 + \frac{37m^4}{20} \right) \frac{2}{3t^2} \right] \sin(\varphi) \\ + \left[\frac{2}{3} + \frac{9m^2}{8} - \left(1 + \frac{7m^2}{4} \right) \frac{1}{2t} + \left(1 + \frac{23m^2}{40} \right) \frac{2}{5t^2} \right] m^2 \sin(3\varphi) \\ - \left(\frac{9}{10} - \frac{1}{t} + \frac{9}{14t^2} \right) \frac{m^4}{4t} \sin(5\varphi) + O(m)^6 \quad (\text{B4}) \end{aligned}$$

for $n = 2$, and

$$\dot{w}_p = \lambda \dot{a} \left\{ \frac{5t}{4} \tan^{-1} [(t-1)^{1/2}] - \left(\frac{11}{4} - \frac{13}{6t} + \frac{2}{3t^2} \right) (t-1)^{1/2} \right\} \sin(\varphi) + O(m)^2 \quad (\text{B5})$$

for $n = 5/2$ for which only the quasi-static limit is given. Finally, the case $n = 3$ is calculated with the following result:

$$\begin{aligned} \dot{w}_p = \lambda \dot{a} \left[\left(2 + 2m^2 + \frac{11m^4}{4} \right) t \log(t) + 6 + 6m^2 + \frac{27m^4}{4} \right. \\ \left. + \left(1 + m^2 + \frac{37m^4}{40} \right) \frac{2}{3t^2} \right] \sin(\varphi) + \left[\left(1 + \frac{55m^2}{32} \right) t - 2 \right. \\ \left. - 27m^2 + (12 + 21m^2) \frac{1}{2t} - (16 + 23m^2) \frac{1}{5t^2} \right] m^2 \sin(3\varphi) \\ - \left(\frac{3t}{4} - \frac{9}{5} + \frac{1}{t} - \frac{3}{7t^2} \right) \frac{3m^4}{8} \sin(5\varphi) + O(m)^6. \quad (\text{B6}) \end{aligned}$$

The particular solutions (B3)–(B6) are all valid only for $t \geq 1$ whereas the homogeneous solutions can be applied in the entire t_x-t_y plane including $t < 1$.

The continuity conditions are that stresses and stress rates are continuous across the elastic plastic boundary [cf. HILL (1961)]. This means that \dot{w} and its first derivative with respect to t are continuous across the boundary $t = 1$. Thus, the constants A_1, B_2 can be determined to

the order of m^4 . After transformation back to the polar coordinates r and θ the following solutions are found:

$$\begin{aligned} \frac{\mu \dot{w}}{\dot{\gamma}_n \tau_n R} = & \left[\left(\frac{\dot{a}}{\alpha \dot{\gamma}_n R} - \frac{1}{3} - \frac{m^2}{2} - \frac{3m^4}{4} \right) \dot{r}^{-1/2} \right. \\ & + \left(1 + \frac{3m^2}{4} + \frac{3m^4}{4} \right) \dot{r}^{1/2} - \left(\frac{2}{3} + \frac{m^2}{4} + \frac{5m^4}{32} \right) \dot{r} \left. \right] \sin \left(\frac{\theta}{2} \right) \\ & + \left[- \left(1 + \frac{3m^2}{2} \right) \dot{r}^{1/2} + \left(\frac{3}{5} + \frac{9m^2}{16} \right) \dot{r} + \frac{m^2}{4} \dot{r}^{3/2} \right] \frac{m^2}{4} \sin \left(\frac{3\theta}{2} \right) \\ & + \frac{5m^4 \dot{r}}{448} \sin \left(\frac{5\theta}{2} \right) + O(m)^6 \end{aligned} \quad (\text{B7})$$

for $n = 1$,

$$\begin{aligned} \frac{\mu \dot{w}}{\dot{\gamma}_n \tau_n R} = & \left[\left(\frac{\dot{a}}{\alpha \dot{\gamma}_n R} - \frac{2}{3} - m^2 - \frac{3m^4}{2} \right) \dot{r}^{-1/2} + 2 + \frac{9m^2}{4} + \frac{91m^4}{32} \right. \\ & - \left(2 + \frac{3m^2}{2} + \frac{3m^4}{2} \right) \dot{r}^{1/2} + \left(\frac{2}{3} + \frac{m^2}{4} + \frac{5m^4}{32} \right) \dot{r} \left. \right] \sin \left(\frac{\theta}{2} \right) \\ & - \left[\frac{5}{3} + \frac{47m^2}{16} - (2 + 3m^2) \dot{r}^{1/2} + \left(\frac{3}{5} + \frac{9m^2}{16} \right) \dot{r} \right. \\ & \left. + \frac{m^2}{6} \dot{r}^{3/2} \right] \frac{m^2}{4} \sin \left(\frac{3\theta}{2} \right) + \left(\frac{7}{5} - \frac{5\dot{r}}{7} \right) \frac{m^4}{64} \sin \left(\frac{5\theta}{2} \right) + O(m)^6 \end{aligned} \quad (\text{B8})$$

or $n = 2$, and finally

$$\begin{aligned} \frac{\mu \dot{w}}{\dot{\gamma}_n \tau_n R} = & \left[\left(1 + \frac{3m^2}{2} + \frac{9m^4}{4} \right) \dot{r}^{-1/2} \log(\dot{r}) \right. \\ & + \left(\frac{\dot{a}}{\alpha \dot{\gamma}_n R} + \frac{11}{3} + \frac{19m^2}{4} + \frac{103m^4}{16} \right) \dot{r}^{-1/2} - 6 - \frac{27m^2}{4} - \frac{273m^4}{32} \\ & + \left(3 + \frac{9m^2}{4} + \frac{9m^4}{4} \right) \dot{r}^{1/2} - \left(\frac{2}{3} + \frac{m^2}{4} + \frac{5m^4}{32} \right) \dot{r} \left. \right] \sin \left(\frac{\theta}{2} \right) \\ & + \left[- (3 + 6m^2) \dot{r}^{-1/2} + 5 + \frac{141m^2}{16} - \left(3 + \frac{9m^2}{2} \right) \dot{r}^{1/2} \right. \\ & \left. + \left(\frac{3}{5} + \frac{9m^2}{16} \right) \dot{r} + \frac{m^2}{8} \dot{r}^{3/2} \right] \frac{m^2}{4} \sin \left(\frac{3\theta}{2} \right) + \left(\dot{r}^{-1/2} - \frac{21}{20} + \frac{5\dot{r}}{28} \right) \frac{m^4}{16} \sin \left(\frac{5\theta}{2} \right) + O(m)^6 \end{aligned} \quad (\text{B9})$$

for $n = 3$.

The solutions in the region $r > R(\theta)$ are

$$\frac{\mu \dot{w}}{\dot{\gamma}_n \tau_n R} = \frac{\dot{a}}{\alpha \dot{\gamma}_n R} \dot{r}^{-1/2} \sin \left(\frac{\theta}{2} \right) - \left(\frac{m^2}{10} + \frac{m^4}{4} \right) \dot{r}^{-1/2} \sin \left(\frac{3\theta}{2} \right) + \frac{3m^4}{112} \dot{r}^{-5/2} \sin \left(\frac{5\theta}{2} \right) + O(m)^6 \quad (\text{B10})$$

for $n = 1$,

$$\frac{\mu \dot{w}}{\dot{\gamma}_o \tau_i R} = \frac{\dot{a}}{\alpha \dot{\gamma}_o R} \hat{r}^{-1/2} \sin\left(\frac{\theta}{2}\right) - \left(\frac{m^2}{15} + \frac{m^4}{6}\right) \hat{r}^{-3/2} \sin\left(\frac{3\theta}{2}\right) + \frac{3m^4}{280} \hat{r}^{-5/2} \sin\left(\frac{5\theta}{2}\right) + O(m)^6 \quad (\text{B11})$$

for $n = 2$, and

$$\frac{\mu \dot{w}}{\dot{\gamma}_o \tau_i R} = \frac{\dot{a}}{\alpha \dot{\gamma}_o R} \hat{r}^{-1/2} \sin\left(\frac{\theta}{2}\right) - \left(\frac{m^2}{10} + \frac{m^4}{4}\right) \hat{r}^{-3/2} \sin\left(\frac{3\theta}{2}\right) + \frac{9m^4}{1120} \hat{r}^{-5/2} \sin\left(\frac{5\theta}{2}\right) + O(m)^6 \quad (\text{B12})$$

for $n = 3$. Because of the cumbersome analysis, inertia terms were never sought for $n = 5/2$.

APPENDIX C: ASYMPTOTIC FIELD CALCULATED WITH PATH INDEPENDENT INTEGRAL

From FREUND and HUTCHINSON (1985) the energy release rate at the crack tip is obtained as follows:

$$G_{\text{tip}} = G - \frac{1}{\dot{a}} \int_A (\tau_{yz} \dot{\gamma}_{yz}^p + \tau_{xz} \dot{\gamma}_{xz}^p) dA - \int_{-R_{\text{max}}}^{R_{\text{max}}} U_e^* dy, \quad (\text{C1})$$

where U_e^* is the residual elastic strain energy density in the remote wake. The plastic zone is denoted A and its largest linear extent in the y -direction is R_{max} . The plastic strain rates $\dot{\gamma}_{xz}^p$ and $\dot{\gamma}_{yz}^p$ are given by

$$\dot{\gamma}_{xz}^p = \frac{\dot{\gamma}_o \tau_i}{\mu} \left(\frac{\tau}{\tau_i} - 1\right)^n \frac{\tau_{xz}}{\tau} \quad \text{and} \quad \dot{\gamma}_{yz}^p = \frac{\dot{\gamma}_o \tau_i}{\mu} \left(\frac{\tau}{\tau_i} - 1\right)^n \frac{\tau_{yz}}{\tau}. \quad (\text{C2})$$

The residual stresses are proportional to the amplitude of the plastic strains, and thus U_e^* is proportional to the squared amplitude of the plastic strains. The last term on the right-hand side of (C1) can therefore be shown to be of the order of λ^2 and will be neglected in the continued analysis. Further

$$\frac{1}{\dot{a}} \int_A (\tau_{yz} \dot{\gamma}_{yz}^p + \tau_{xz} \dot{\gamma}_{xz}^p) dA = \frac{1}{\dot{a}} \int_A \frac{\dot{\gamma}_o \tau_i}{\mu} \left(\frac{\tau}{\tau_i} - 1\right)^n \tau dA = \frac{\dot{\gamma}_o \tau_i}{\mu \dot{a}} \int_{-\pi}^{\pi} \int_0^{R_p(\theta)} \left[\frac{\tau(r)}{\tau_i} - 1\right]^n \tau(r) r dr d\theta. \quad (\text{C3})$$

The distance to the elastic plastic boundary is given by (A2). The integration with respect to r is changed to integration with respect to τ . The following is obtained:

$$\frac{1}{\dot{a}} \int_A (\tau_{yz} \dot{\gamma}_{yz}^p + \tau_{xz} \dot{\gamma}_{xz}^p) dA = \frac{\dot{\gamma}_o \tau_i K_{\text{tip}}^4}{2\pi^2 \mu \dot{a}} \int_{-\pi}^{\pi} \left[\frac{R_p(\theta)}{R_p(0)}\right]^2 d\theta \int_{\tau_i}^{\infty} \left(\frac{\tau}{\tau_i} - 1\right)^n \tau^{-4} d\tau. \quad (\text{C4})$$

Writing becomes simplified after the introduction of

$$g(m) = \frac{1-m^2}{2\pi m} \int_{-\pi}^{\pi} \left[\frac{R_p(\theta)}{R_p(0)}\right]^2 d\theta = \frac{8-8m^2+3m^4}{8m(1-m^2)^{3/2}} \quad (\text{C5})$$

and

$$\delta = \frac{3\tau_i^3}{\pi} \int_{\tau_i}^{\infty} \left(\frac{\tau}{\tau_i} - 1\right)^n \tau^{-4} d\tau = \begin{cases} \frac{1}{2\pi} & \text{for } n = 1, \\ \frac{1}{\pi} & \text{for } n = 2, \\ \frac{15}{16} & \text{for } n = \frac{5}{2}. \end{cases} \quad (\text{C6})$$

Inserted into (C1), this gives a relation between the elastic energy release rate G and the crack-tip driving force G_{tip} :

$$G_{\text{tip}}/G = 1 - \delta g(m) \frac{\dot{\gamma}_0 (\mu \rho)^{1/2} G_{\text{tip}}}{3\tau_i^2}, \quad (\text{C7})$$

or, to relate K_{III} and K_{tip} ,

$$K_{\text{tip}}/K_{\text{III}} = 1 - \delta \frac{g(m)}{(1-m^2)^{1/2}} \frac{\dot{\gamma}_0 \rho^{1/2} K_{\text{tip}}^2}{6\tau_i^2 \mu^{1/2}}. \quad (\text{C8})$$

Equations (C7) and (C8) are accurate to the order of λ^2 .